



ELSEVIER

Available online at [www.sciencedirect.com](http://www.sciencedirect.com)

SCIENCE @ DIRECT®

International Journal of Multiphase Flow 31 (2005) 793–808

International Journal of  
**Multiphase  
Flow**

[www.elsevier.com/locate/ijmulflow](http://www.elsevier.com/locate/ijmulflow)

## Particle mixing in a sheared granular flow

Shu-San Hsiau <sup>\*</sup>, Li-Shin Lu, Juin-Chung Chen, Wen-Lung Yang

*Department of Mechanical Engineering, National Central University, Chung-Li 32054, Taiwan, ROC*

Received 8 February 2004; received in revised form 21 February 2005

---

### Abstract

Mixing experiments were performed in a shear cell device using differently colored but otherwise identical glass spheres, with five different bottom wall velocities. The motions of the granular materials were recorded by a high-speed camera, so the development of mixing boundaries could be analyzed from the images. By continually tracking the movements of particles, the velocity, fluctuations and the granular temperatures were measured. The self-diffusion coefficients were determined from the histories of particles movements. The mixing layer thicknesses were compared with the calculations from a simple diffusion equation using the data of self-diffusion coefficients obtained from the current measurements. The calculations and experimental results showed good agreements, demonstrating that the mixing process of granular materials occurred through the diffusion mechanism.

© 2005 Elsevier Ltd. All rights reserved.

*Keywords:* Granular flow; Shear cell; Mixing; Diffusion; Image processing; Velocity fluctuation

---

### 1. Introduction

A granular flow is a two-phase flow with collections of discrete solid particles dispersed in an interstitial fluid, where the gaseous phase plays a negligible role in the flow mechanics. The dominant mechanism affecting the flow behavior of granular materials is the random motions of particles resulting from the interactive collisions between particles (Campbell, 1990). Because the

---

<sup>\*</sup> Corresponding author. Tel.: +886 3 426 7341; fax: +886 3 425 4501.

*E-mail address:* [sshsiau@cc.ncu.edu.tw](mailto:sshsiau@cc.ncu.edu.tw) (S.-S. Hsiau).

random motions of particles in a granular flow are analogous to the motion of molecules in a gas, the dense-gas kinetic theory (Savage and Jeffrey, 1981; Jenkins and Savage, 1983; Lun et al., 1984; Jenkins and Richman, 1985) and molecular dynamic simulations (Walton and Braun, 1986; Campbell, 1989; Lan and Rosato, 1995) are used to analyze and model the granular flow behavior.

The random motions of particles are quantified by granular temperature, which is defined as the specific fluctuation kinetic energy of particles and serves as a key property of granular material flows (Ogawa, 1978). In dense-gas kinetic theory, the granular temperature is assumed to be isotropically distributed. However, this key assumption may fail in most granular material flow systems (Campbell, 1990), where the granular temperature plays the same role as the thermodynamic temperature in a gas. The energy of granular temperature is continually dissipated through the inelastic collisions between particles or between particles and boundaries. Thus the external energy must be continually input into the system to maintain the granular temperature.

Mixing of granular materials has economical importance in different industries, such as foodstuffs, pharmaceutical products, detergents, chemicals, plastics etc. In many cases a better mixing process could tremendously increase the quality and the value of product. Thus mixing is regarded as a key process and needs further study. However, mixing of granular materials has received less attention than fluids (Ottino and Khakhar, 2000), although the subject of granular mixing in several kinds of mixers has drawn the interest of several researchers in recent years. The convective and dispersive mixing mechanisms in a rotating tumbler (McCarthy et al., 2000), in a V-blender (Moakher et al., 2000) and in a tote blender (Sudah et al., 2002) had been examined by both experimental tests and computer simulations. The mixing rate in a cylindrical bladed mixer was shown to be enhanced by increasing the blade speed (Zhou et al., 2003). From several experimental studies, it was demonstrated that the mixing process occurred through a diffusion mechanism in different transport devices, e.g., in an inclined chute (Hwang and Hogg, 1980), in a shear apparatus (Scott and Bridgewater, 1976; Buggish and Löffelmann, 1989; Hsiau and Shieh, 1999), in a vertical channel (Hsiau and Hunt, 1993a; Natarajan et al., 1995) and in a vibrated bed (Zik and Stavans, 1991; Hunt et al., 1994). Besides, computer simulation has become a powerful tool to study the mixing behaviors in a granular flow system. A detailed study of granular mixing using computer simulations demonstrated that the amount and nature of the mixing was quite sensitive to a range of physical properties (Cleary et al., 1998). The influence of granular temperature gradient on the mixing condition was examined by Henrique et al. (2000), also using computer simulation.

The Couette granular flow is considered as one of the simplest flow models and very suitable for fundamental research (Savage and Mckeown, 1983; Savage and Sayed, 1984; Hanes and Inman, 1985; Johnson and Jackson, 1987; Wang and Campbell, 1992; Hsiau and Yang, 2002). However, there have been relatively few studies discussing the mixing process in a Couette granular flow. The present paper uses image technology to investigate the granular flow mixing behaviors in a shear cell. The dependences of mixing developments on diffusion coefficients, granular temperature and shear rate are discussed.

## 2. Experimental setup and technique

A rotating shear cell was constructed to generate the shear granular flow, as shown in Fig. 1. The shear device consists of a bottom disk and an upper disk. The bottom disk, with outside

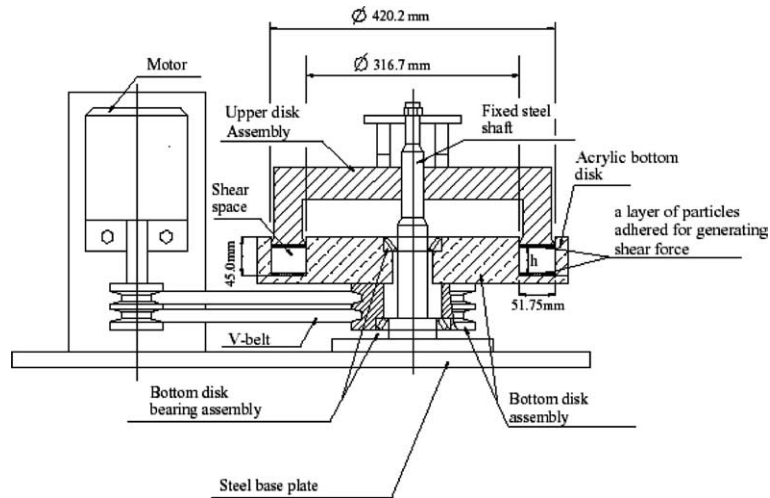


Fig. 1. The schematic drawing of the experimental apparatus.

diameter of 45.00 cm, is driven by a 3 hp AC motor. The rotation speed is controlled by a variable speed inverter and can be measured by a tachometer. The bottom disk is made of plexiglass for observation. An annular trough (inside diameter: 31.67 cm; outside diameter: 42.02 cm; depth: 4.5 cm) was cut in the bottom disk. The stationary upper disk could be inserted into the trough where the granular materials are put in the test section. The test section height  $2h$  could be adjusted and measured by a dial indicator.

Soda lime beads (colors of black and white) with an average diameter  $d_p$  of 2 mm (standard deviation of 0.04 mm and particle density of  $2508 \text{ kg/m}^3$ ) were used as granular materials in the experiments. In the mixing experiments, 1.15 kg of black particles were carefully put in the bottom half of the text section and then 1.15 kg of white particles were put above. The average solid fraction of the test is calculated from the particle mass (2.30 kg in this paper) divided by the particle density and the test section volume. A layer of 3 mm soda lime beads was adhered to both the bottom and the top surfaces, in a random packing organization.

The granular flow in the test section is assumed to be two-dimensional with streamwise (horizontal) direction as  $x$ -axis and transverse (vertical) direction as  $y$ -axis (upwards is positive). Because of the limitations on observation, only the flows adjacent to the outer surface of the annular trough in the bottom disk could be recorded and analyzed. The inner surface was cleaned and polished before each experiment to reduce the wall friction effect. The velocity at the bottom (outside lower corner of the trough)  $u_0$  could be calculated from the product of the rotational speed of the bottom disk and the outside radius of the trough.

The mixing process was recorded by a high-speed camera (Kodak motion corder analyzer with highest speed of 10,000 frames per second). The frames were digitized to gray levels (ranging from 0 to 255 due to the different colors of the black and the white particles) and stored in a computer file. The test section was divided into 120 altitudes along the transverse direction. Using image processing, the concentrations of white particles  $C(t)$  in each altitude were determined. The mixing layer thickness  $\delta(t)$  is defined from the width with concentrations ranging from 0.05 to 0.95, as

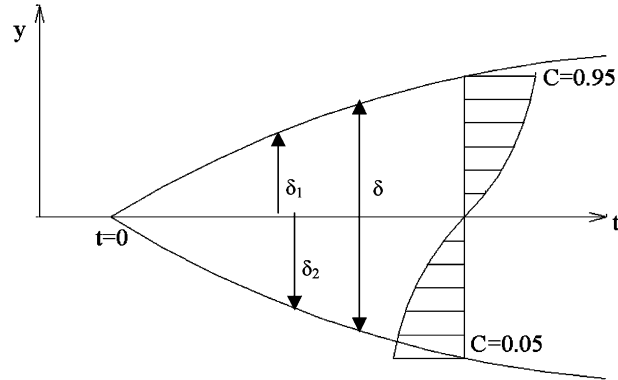


Fig. 2. Schematic representation of the boundary layer thickness developed in the Couette shear cell.

shown in Fig. 2. The symbols  $\delta_1(t)$  and  $\delta_2(t)$  denote the thicknesses of the mixing layer of the upper and the lower parts, respectively.

To investigate the diffusion process, the fluctuation velocities and self-diffusion coefficients were also determined from the experiments by different combinations of colored particles: The black particles served as tracer particles and about 15% of black particles were mixed uniformly with 85% of white particles. All the experimental settings were the same as the mixing experiment, except for the arrangement of colored particles. The autocorrelation technique was employed to process the stored images and to decide the shift of each tracer particle in every two consecutive images. The details of the autocorrelation process can be referred to the paper by Hsiau and Shieh (1999).

The test section was vertically divided into 10 regions in the experiment of fluctuation velocity. By averaging about 250 tracer particles' velocities from approximately 8500 frames, the overall average velocities in horizontal and vertical directions,  $\langle u \rangle$  and  $\langle v \rangle$ , in each region were determined. The fluctuation velocities in the two directions,  $\langle u'^2 \rangle^{1/2}$  and  $\langle v'^2 \rangle^{1/2}$ , for each region were defined by the mean square root of the deviations of each local velocity from the overall average velocity. The granular temperature  $T$  was used to quantify the kinetic energy of the flow, and could be calculated from the average of the mean square of the fluctuation velocities in two directions.

Since the current study followed the auto-correlation technique developed by Hsiau and Shieh (1999) which considered the correlation values of gray level derivatives, the experimental errors of the velocities were reduced to within 1.5%.

The velocity fluctuations induce the self-diffusion in granular shear flows. Einstein (1956) first employed this concept to analyze the diffusive phenomena of suspended particles with Brownian motion in a liquid. This idea was also used by Savage and Dai (1993) and by Campbell (1997) to investigate the diffusive behavior of granular flow systems through computer simulation. The self-diffusion coefficient  $D_{ij}$  was defined as

$$\lim_{t \rightarrow \infty} \langle \Delta x_i \Delta x_j \rangle = 2D_{ij}t \quad (1)$$

where  $\Delta x_i$  and  $\Delta x_j$  are the diffusive displacements in directions  $i$  and  $j$ . A similar concept was employed in experiments by Natarajan et al. (1995) to study the granular self-diffusion in a

1-m-high vertical channel, and by Hsiau and Shieh (1999) to study the diffusion in a shear cell. In order to obtain longer histories of particle movements in a Couette device through a small camera window, the idea of “periodic cell” used in computer simulation (Campbell and Brennen, 1985) was proposed for application in experiments by Hsiau and Shieh (1999). In the periodic cell used in computer simulation, when a particle leaves the cell, a new particle with the same velocity will be set at the same transverse position in the cell inlet. Employing this idea for an experiment, when a tracer particle moved out of one image, the time counter for this particle paused until another tracer particle entered the cell inlet with the same channel height and the same velocity as the previous tracer particle. The path of this new tracer particle from the image inlet was then treated as the continuous movements of the former tracer particle. Details can be found in the paper by Hsiau and Shieh (1999), and the current study follows the same approach. Since the current mixing experiments were mainly resulted to the diffusion in the transverse direction, which were evaluated in this study. The mean-square diffusive displacements in the transverse direction  $\langle \Delta y \cdot \Delta y \rangle$  were averaged from about 200 tracer particles taken from 6000 to 9000 frames. The experimental errors resulted mainly from the uncertainty in determining the centroid of a particle. The errors of diffusion coefficients  $D_{yy}$  were estimated within 5%.

### 3. Results and discussions

Every test in this study was done for a total granular mass of 2.30 kg and a fixed channel height ( $2h$ ) of 2.5 cm. Hence the average solid fraction of the channel was a constant, 0.6178. In the experiments of this study, five bottom wall velocities  $u_0$ , 0.66 m/s, 0.88 m/s, 1.10 m/s, 1.32 m/s and 1.54 m/s, were used to investigate the variations of the mixing layer thickness. The results of experiments were also compared with calculations from the diffusion equation. Meanwhile, the properties concerned with the development of mixing layer, for example, the mixing growing rate, the apparent self-diffusion coefficient, the granular temperature and the shear rate, were studied to explore the characteristics of mixing phenomena in the shear cell.

Fig. 3 shows the distributions of the overall average velocities in the streamwise and transverse directions,  $\langle u \rangle$  and  $\langle v \rangle$ , with  $u_0$  of 0.66 m/s, 0.88 m/s, 1.10 m/s, 1.32 m/s and 1.54 m/s. As expected, the transverse velocities are close to 0 because there is no vertical bulk motion in the channel. The streamwise velocity decreases with the channel height. The streamwise velocity is greater for the case with greater bottom wall velocity, consistent with the results of Hsiau and Shieh (1999). Fig. 4 shows the fluctuation velocity distributions in the channels for the five cases. The fluctuations are not isotropic, and the values in the streamwise direction are larger. The explanation for this anisotropic phenomenon can be found in Hsiau and Shieh (1999). Because of the increase in the shear rate ( $d\langle u \rangle/dy$ ) with the height, the fluctuations in both directions also increase with the channel height, as shown in Fig. 4. The flow with the greater bottom wall velocity induces relatively greater fluctuations in both directions, due to the higher shear rates. It is noted that the streamwise velocity fluctuations are greater than the transverse velocity fluctuations, however, for the study of the top-bottom mixture in the shear cell, the transverse velocity fluctuations play a much more important role to influence the granular mixing, than does the streamwise velocity fluctuation.

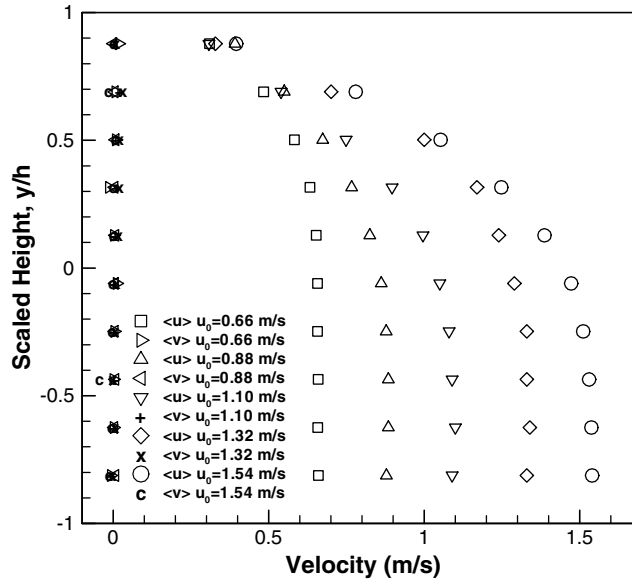


Fig. 3. The distributions of overall average velocity in the streamwise  $\langle u \rangle$  and transverse  $\langle v \rangle$  directions.

The channel can be divided into two flow regimes: the “fluid-like regime” in the upper section and the “solid-like regime” in the lower section (Zhang and Campbell, 1992), due to the scale of the shear rate. In this paper, the same particles but with different colors are initially arranged in the top-bottom organization to investigate the particle mixing in the shear cell. Thus, the test section is also divided into two regions, the upper channel ( $y > 0$ ) and the lower channel ( $y < 0$ ). To

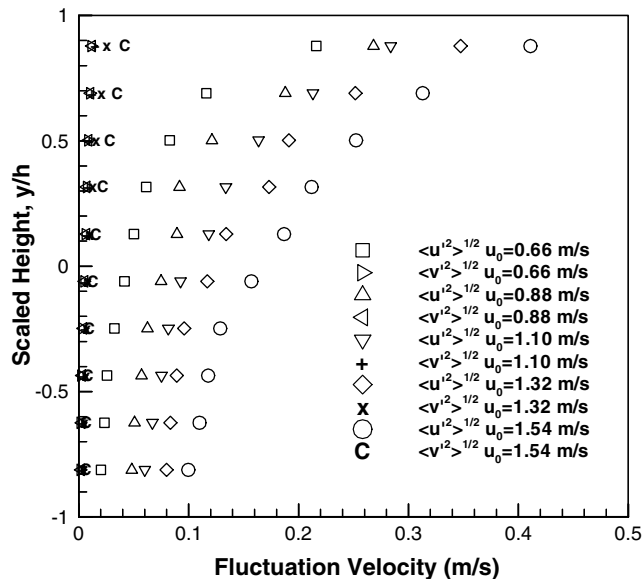


Fig. 4. The distributions of fluctuation velocities in the streamwise  $\langle u'^2 \rangle^{1/2}$  and transverse  $\langle v'^2 \rangle^{1/2}$  directions.

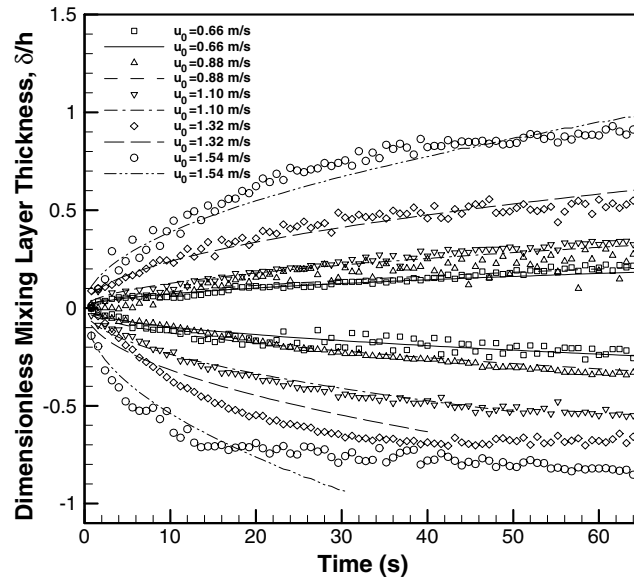


Fig. 5. The evolution of the experimental boundary layer thicknesses (symbols) with the five tests ( $u_0 = 0.66$  m/s, 0.88 m/s, 1.10 m/s, 1.32 m/s and 1.54 m/s). Curves are best fit to Eqs. (5) and (6) described in text.

examine the influence of the bottom wall velocity on the development of the mixing layer, Fig. 5 shows the developments of the mixing layer thickness with time for the five tests with different bottom wall velocities. Note that the mixing layer thickness in Fig. 5 is non-dimensionalized by the half channel height,  $h$ . It is clear that the mixing layers expand with time and develop faster in the initial stages. The mixing layer thicknesses of the upper channel,  $\delta_1$  are slightly greater than those of the lower channel,  $\delta_2$ . Moreover, the influence of wall velocity on the development of mixing layer is significant. From this figure, the mixing layer thicknesses are greater for the cases with the greater bottom wall velocity.

In all tests shown in Fig. 5, the mixing layer thicknesses in both upper and lower parts developed much faster in the beginning stages, and then grew smoothly. The mixing growing rates,  $R$ , can be measured by differentiating the mixing layer thicknesses ( $\delta_1$  and  $\delta_2$ ) with respect to time. The mixing growing rates of the upper and lower channels are calculated from the experimental data in Fig. 5 and are plotted against time for the five bottom wall velocities in Fig. 6(a) and (b) for the upper and lower channels, respectively. It is evident that the mixing growing rates are greater in the initial stage. It is also shown that the mixing growing rates increase with the increasing bottom wall velocity. Meanwhile, most of the mixing growing rates in the upper channel (Fig. 6(a)) are greater than those in the lower channel (Fig. 6(b)) since the fluid-like behavior of the granules in the upper channel promote the granular mixing easier.

Granular mixing mainly resulted from the diffusive motions of granular materials in the shear cell. Because of the top-bottom organization of different-colored particles, the particle mixing occurred in the vertical direction. Thus the diffusion equation can be written as

$$\frac{\partial C}{\partial t} = \frac{\partial}{\partial y} \left( D_{yy} \frac{\partial C}{\partial y} \right) \quad (2)$$

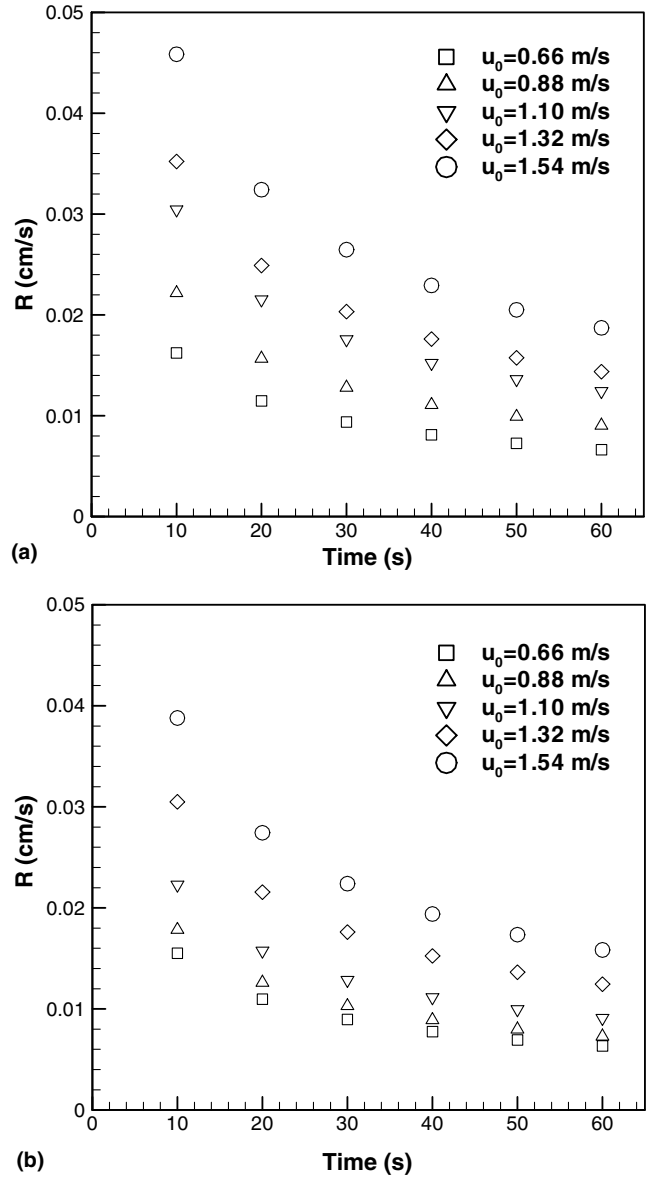


Fig. 6. The mixing growing rates  $R$  varied with time for five bottom wall velocities (a) in the upper channel, (b) in the lower channel.

where  $C$  is the concentration of white particles, and  $D_{yy}$  is the transverse self-diffusion coefficient. The initial conditions are  $C = 1$  when  $t = 0, y > 0$ ; and  $C = 0$  when  $t = 0, y < 0$ . Since the mixing layer thicknesses almost stop growing after a certain time (60 s), even with longer observation of the mixing process up to a half hour, the mixing boundary layer had not reached the walls. Thus it is reasonable to assume the boundary conditions for the above equation as:  $C \rightarrow 1$  as  $y \rightarrow \infty$ ; and  $C \rightarrow 0$  as  $y \rightarrow -\infty$ . The transverse self-diffusion coefficients  $D_{yy}$  is actually varied with the height



of the channel in the experimental results, which will be investigated later. However, in order to get the analytical solution,  $D_{yy}$  in Eq. (2) can be assumed as constants: apparent self-diffusion coefficients  $D_{app,1}$  and  $D_{app,2}$  to explore the bulk mixing behavior in the upper and lower channels respectively. In fact, the apparent self-diffusion coefficients denote the “averaged” self-diffusion in the upper and lower channels. Thus, we solve Eq. (2) for the regions of  $y \geq 0$  (upper channel) and  $y \leq 0$  (lower channel) with one additional boundary condition by assuming  $C \rightarrow 0.5$  at  $y = 0$ . Then, the analytical solutions of Eq. (2) are

$$C(t, y) = \frac{1}{2} + \frac{1}{2} \operatorname{erf} \left( \frac{y}{2\sqrt{D_{app,1}t}} \right) \quad (\text{for upper channel}) \tag{3}$$

$$C(t, y) = \frac{1}{2} - \frac{1}{2} \operatorname{erf} \left( \frac{y}{2\sqrt{D_{app,2}t}} \right) \quad (\text{for lower channel}) \tag{4}$$

According to the definition of mixing layer thickness in the experiments,  $C = 0.95$  at  $y = \delta_1$  and  $C = 0.05$  at  $y = -\delta_2$ , that gives

$$\delta_1 = 2.53\sqrt{D_{app,1}t} \quad (\text{for upper channel}) \tag{5}$$

$$\delta_2 = 2.53\sqrt{D_{app,2}t} \quad (\text{for lower channel}) \tag{6}$$

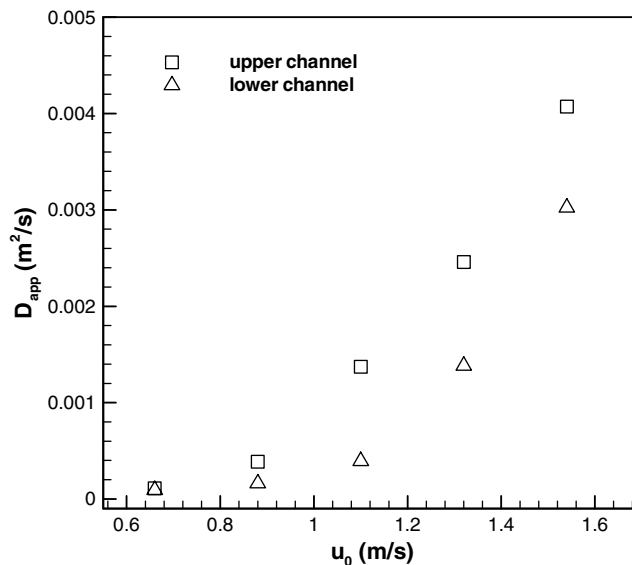


Fig. 7. The dependence of the apparent self-diffusion coefficient  $D_{app}$  on the bottom wall velocity  $u_0$  both in the upper and lower channels.

The fitted curves in Fig. 5 are the results of least-squares fits using the forms of Eqs. (5) and (6), indicating close correspondence with the experimental data. The deviations are due to the assumption of constant self-diffusion coefficients in the upper and lower channels in the diffusion equation.

The values of the apparent diffusion coefficients can be determined from the fitted curves (Eqs. (5) and (6)) in Fig. 5. The dependences of the apparent diffusion coefficients on the bottom wall velocity are shown in Fig. 7. It is clearly that  $D_{app}$  increase with the increasing bottom wall velocity. Besides, the apparent self-diffusion coefficients in the upper channel are greater than those in the lower channel, indicating a better mixing in the upper channel. Compared with the results of Fig. 5, it is not surprised that the mixing layer thicknesses increase with the increasing bottom wall velocity. In addition, the mixing layer thicknesses of the upper part are greater (Fig. 5) since the apparent self-diffusion coefficients are greater. Therefore, the apparent self-diffusion coefficient  $D_{app}$  is an appropriate index to describe the “averaged” granular mixing condition in the shear cell.

As mentioned above, the granular temperature is an important property to quantify the kinetic energy of particles. Thus, the diffusive motions of granular materials are related to the granular temperature. Fig. 8 shows the apparent self-diffusion coefficients plotted against the square root of the average granular temperature in the vertical direction,  $T_y^{1/2}$  (the average of the vertical fluctuation velocities), in the upper and lower channels, where the granular temperatures are measured from the tests with five different bottom wall velocities. It is shown that the granular temperatures in the upper and lower channels clearly increase with the increasing bottom wall velocity. Furthermore, the granular temperature in the upper channel is much greater than that in the lower channel with the same bottom wall velocity, which is also indicated in Fig. 4. The

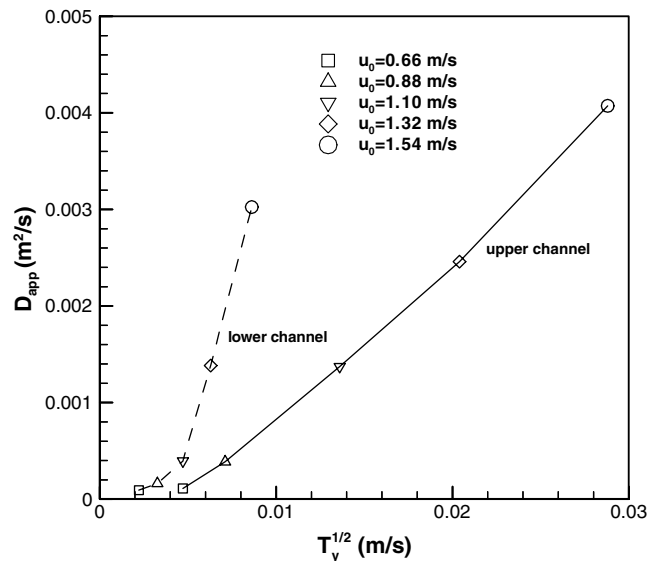


Fig. 8. The apparent self-diffusion coefficients versus the square root of the average granular temperature in the vertical direction,  $T_y^{1/2}$ , in the upper and lower channels.

apparent diffusion coefficient  $D_{app}$  increases linearly and significantly with the square root of the vertical granular temperature in the upper channel, where granular materials behave like a fluid. The linear dependence was also derived from the dense-gas kinetic theory by Hsiau and Hunt (1993b) and Savage and Dai (1993). However the theoretical values of the self-diffusion coefficient are much smaller than the experimental results. The deviation is up to an order of 2–3. The significant deviations are mainly resulted from the assumptions in the dense-gas kinetic theory: the isotropic and binary collisions, the isotropic fluctuations and granular temperature. In addition, the linear dependence of  $D_{app}$  on  $T_y^{1/2}$  in the lower channel is relatively weak, because the gravity effect causes a solid-like behavior resulting in a much larger deviations from the dense-gas kinetic theory derivation.

The granular temperature and the diffusion coefficient are mainly influenced by the shear rate along the (upper) wall (Hsiau and Yang, 2002). Fig. 9 shows the apparent self-diffusion coefficient versus the shear rate along the upper wall,  $\langle du/dy \rangle_w$ , with five bottom wall velocities. The values of shear rates along the upper wall are extracted from the velocity distributions in Fig. 3. The value of the shear rate is greatest in the test with fastest bottom wall velocity. Meanwhile, the greater shear rate induces stronger diffusion with the greater apparent self-diffusion coefficient, as shown in Fig. 9. The apparent diffusion coefficient shows a good correlation with the shear rate.

In fact, the self-diffusion coefficient was varied with the height of the channel due to the characteristics of granular motions in the test section, as demonstrated in the papers of Hsiau and Shieh (1999) and Hsiau and Yang (2002). Following the experimental procedures in Hsiau and Shieh (1999), the transverse self-diffusion coefficients  $D_{yy}$  were measured. Fig. 10 shows the distributions of the transverse self-diffusion coefficient in the test channel with five different bottom

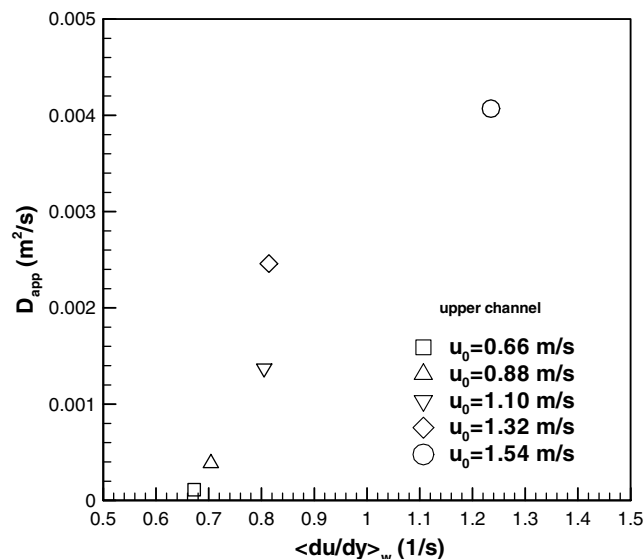


Fig. 9. The apparent self-diffusion coefficient  $D_{app}$  versus the shear rate along the upper wall,  $\langle du/dy \rangle_w$ , with five bottom wall velocities.

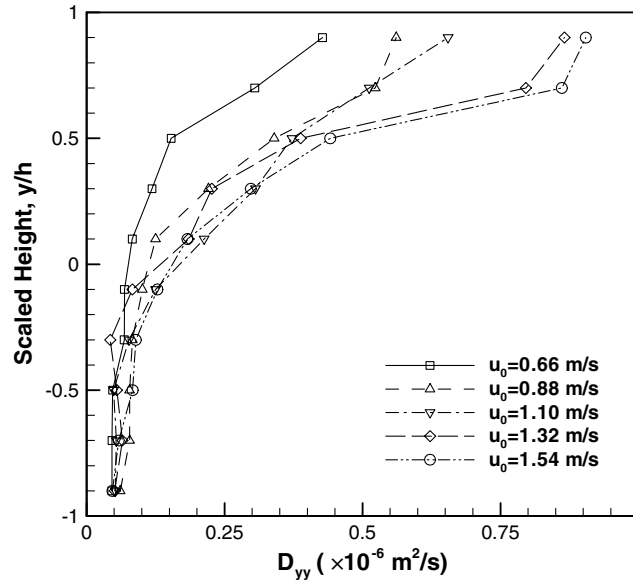


Fig. 10. The distributions of the experimental transverse self-diffusion coefficient  $D_{yy}$  with five bottom wall velocities.

wall velocities. The self-diffusion coefficients in the upper channel ( $y > 0$ ) are much greater than those in the lower channel ( $y < 0$ ). Due to the effect of gravity, the particles in the lower part are pressed by greater gravitational force from the upper particles, so the granular structures of lower part are denser. As shown in Fig. 3 and explained above, this regime is characterized as a solid-like region. Both the granular fluctuation movements and shear rates increase with the channel height from the bottom to the top, as shown in Figs. 3 and 4. Thus the greater fluctuations and shear rates induce the stronger diffusion in the upper channel. It is also shown in Fig. 10 that the transverse diffusion coefficient  $D_{yy}$  increases with the increasing bottom wall velocity, due to higher energy input into the granular system when the bottom wall moves faster.

For greater accuracy, the diffusion equation (Eq. (2)) can be solved by the finite difference method where the measured transverse diffusion coefficients  $D_{yy}$  are employed. Here, the channel is divided into 10 subregions vertically and the values of transverse self-diffusion coefficient,  $D_{yy}$ , in each subregion are extracted from the current experimental results in Fig. 10. The initial conditions are the same as the previous ones, while the boundary conditions are

$$\left(\frac{\partial C}{\partial y}\right)_{y=\pm h} = 0 \quad (7)$$

since there is zero mass flux through the walls. Then, the concentration  $C$ , at each level can be calculated from the finite difference equations. Fig. 11(a)–(c) show the concentration distributions in the channel at times of 10, 20, 30, 40, 50 and 60 s, from both the experimental measurements and the numerical solutions for the bottom wall velocities of 0.66 m/s, 1.10 m/s and 1.54 m/s. Generally, a perfect mixing condition means that the concentrations in all levels are 0.5, although

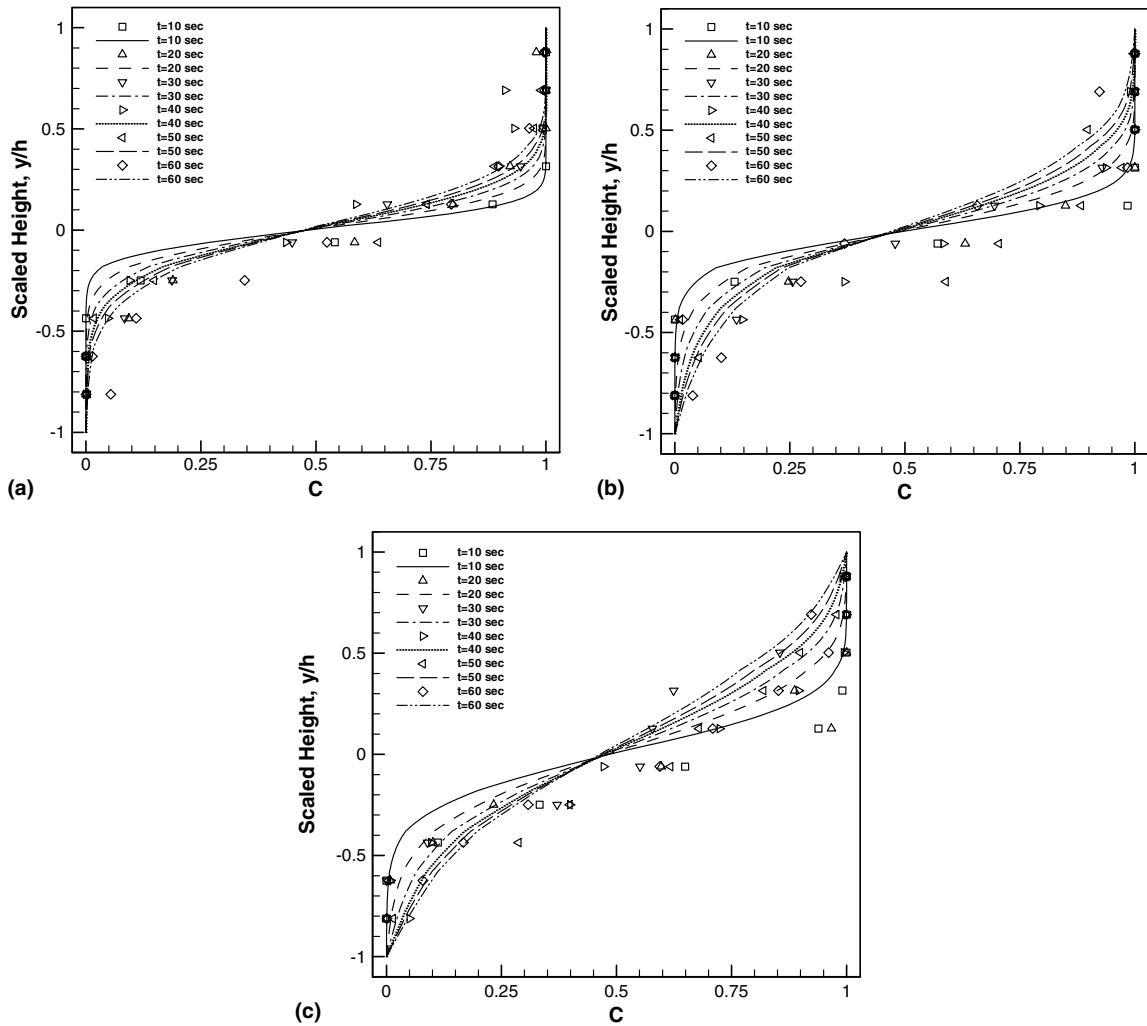


Fig. 11. The concentration distributions of both the experimental measurements (symbols) and the numerical solutions (curves) at times of 10, 20, 30, 40, 50 and 60 s: (a)  $u_0 = 0.66$  m/s, (b)  $u_0 = 1.10$  m/s, (c)  $u_0 = 1.54$  m/s.

this is almost impossible in an actual situation. Therefore, the smaller concentration gradient in the channel indicates that the mixture is more homogeneous with better mixing conditions. From these figures, the greater bottom wall velocity results a smaller concentration gradient along the height, indicating that the greater bottom wall velocity causes better mixing in the channel. Fig. 11(a)–(c) also show the deviations between experiments and numerical results are larger in the central channel, which is due to the difficulty in determining the concentration accurately in this region.

The semi-theoretical mixing layer thickness can be calculated by the combination of the numerical solutions of concentration along the height and the definition of the mixing layer thickness, as mentioned above. Fig. 12 shows the semi-theoretical results compared with the experimental data

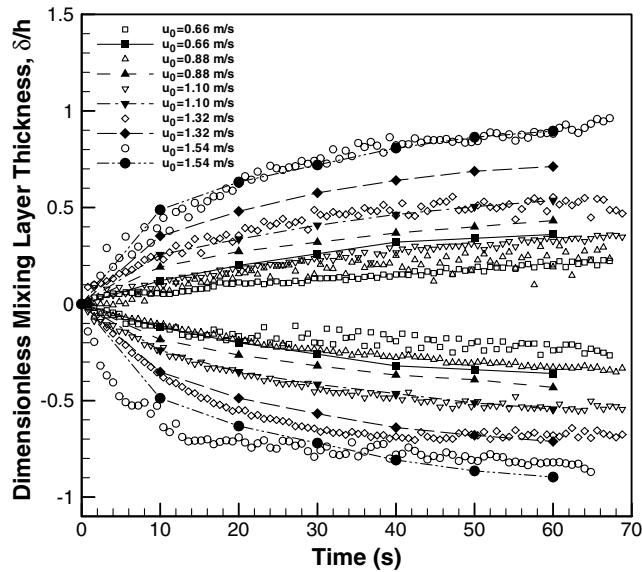


Fig. 12. Comparison between the experimental data (open symbols) and the semi-theoretical results (closed symbols with lines) of the evolution of the mixing layer thickness under five bottom wall velocities.

for the mixing layer thickness non-dimensionalized by the half channel height. The comparison shows a very good agreement, indicating that the mixing process of granular materials in the shear cell occurred throughout the diffusion mechanism.

#### 4. Conclusions

This paper studies the mixing behavior of granular materials in a two-dimensional shear cell. The image processing technology and a particle tracking method were employed to measure the fluctuation velocities, the mixing layer thicknesses, the granular temperatures and the self-diffusion coefficients. Five conditions with different bottom wall velocities (0.66 m/s, 0.88 m/s, 1.10 m/s, 1.32 m/s and 1.54 m/s) were tested. The diffusion equation is used to investigate the mixing mechanism in the test section.

The shear rate was found to increase with the increasing bottom wall velocity. The high velocity fluctuations in the upper channel were caused by the large shear rate along the upper wall. The high velocity fluctuations induced both a greater self-diffusion coefficient and the granular temperature in the upper channel. Therefore, the mixing layer thickness was greater and the mixing growing rate was faster in the upper part of the test section.

An important result of this study was determining the apparent self-diffusion coefficient from the mixing layer thickness. The apparent self-diffusion coefficient could appropriately describe the mixing behaviors in the channel. The apparent self-diffusion coefficient was shown to depend linearly on the square root of the transverse granular temperature in the fluid-like regime, as derived from the dense-gas kinetic theory. Also, the semi-theoretical mixing layer thickness, calculated from the diffusion equation by substituting the measured self-diffusion coefficient, agreed

well with the experimental data, indicating that the particle mixing in the shear cell was governed by the diffusive mechanism.

## Acknowledgement

Financial support from the National Science Council of the ROC for this work through project NSC 91-2212-E-008-033 and NSC 92-2212-E-008-007 is gratefully acknowledged.

## References

- Buggish, H., Löffelmann, G., 1989. Theoretical and experimental investigation into local granulate mixing mechanism. *Chem. Eng. Process.* 26, 193–200.
- Campbell, C.S., 1989. The stress tensor for simple shear flow of a granular material. *J. Fluid Mech.* 203, 449–473.
- Campbell, C.S., 1990. Rapid granular flows. *Annu. Rev. Fluid Mech.* 22, 57–92.
- Campbell, C.S., 1997. Self-diffusion in granular shear flows. *J. Fluid Mech.* 348, 85–101.
- Campbell, C.S., Brennen, C.E., 1985. Computer simulation of granular shear flows. *J. Fluid Mech.* 151, 167–188.
- Cleary, P.W., Metcalfe, G., Liffman, K., 1998. How well do discrete element granular flow models capture the essentials of mixing processes. *Appl. Math. Model.* 22, 995–1008.
- Einstein, A., 1956. *Investigations on the Theory of Non-Uniform Gases*. Dover Publ. Co., New York, Chapter 1, pp. 12–27.
- Hanes, D.M., Inman, D.L., 1985. Observations of rapid flowing granular-fluid flow. *J. Fluid Mech.* 150, 357–380.
- Henrique, C., Batrouni, G., Bideau, D., 2000. Diffusion as a mixing mechanism in granular materials. *Phys. Rev. E* 6301, 1304.
- Hsiau, S.S., Hunt, M.L., 1993a. Shear-induced particle diffusion and longitudinal velocity fluctuations in a granular-flow mixing layer. *J. Fluid Mech.* 251, 299–313.
- Hsiau, S.S., Hunt, M.L., 1993b. Kinetic theory analysis of flow-induced particle diffusion and thermal conduction in granular material flows. *Trans. ASME C: J. Heat Transf.* 115, 541–548.
- Hsiau, S.S., Shieh, Y.H., 1999. Fluctuations and self-diffusion of sheared granular material flows. *J. Rheol.* 43, 1049–1066.
- Hsiau, S.S., Yang, W.L., 2002. Stresses and transport phenomena in sheared granular flows with different wall conditions. *Phys. Fluids* 14, 612–621.
- Hunt, M.L., Hsiau, S.S., Hong, K.T., 1994. Particle mixing and volumetric expansion in a vibrated granular bed. *J. Fluids Eng.* 116, 785–791.
- Hwang, C.L., Hogg, R., 1980. Diffusive mixing in flowing powders. *Powder Technol.* 26, 93–101.
- Jenkins, J.T., Richman, M.W., 1985. Kinetic theory for plane flows of a dense gas of identical, rough, inelastic, circular disks. *Phys. Fluids* 28, 3485–3494.
- Jenkins, J.T., Savage, S.B., 1983. A theory for the rapid flow of identical, smooth, nearly elastic, particles. *J. Fluid Mech.* 130, 187–202.
- Johnson, P.C., Jackson, R., 1987. Frictional-collisional constitutive relations for granular materials, with application to plane shearing. *J. Fluid Mech.* 176, 67–93.
- Lan, Y., Rosato, A.D., 1995. Macroscopic behavior of vibrating beds of smooth inelastic spheres. *Phys. Fluids* 7, 1818–1831.
- Lun, C.K.K., Savage, S.B., Jeffrey, D.J., Chepur, N., 1984. Kinetic theories for granular flow: inelastic particles in Couette Flow and slightly inelastic particles in a flow field. *J. Fluid Mech.* 140, 233–256.
- McCarthy, J.J., Khakhar, D.V., Ottino, J.M., 2000. Computational studies of granular mixing. *Powder Technol.* 109, 72–82.
- Moakher, M., Shinbrot, T., Muzzio, F.J., 2000. Experimentally validated computations of flows, mixing and segregation of noncohesive grains in 3D tumbling blenders. *Powder Technol.* 109, 58–71.

- Natarajan, V.V.R., Hunt, M.L., Taylor, E.D., 1995. Local measurements of velocity fluctuations and diffusion coefficients for a granular material flow. *J. Fluid Mech.* 304, 1–25.
- Ogawa, S., 1978. Multi-temperature theory of granular materials. In: *Proceedings of US-Japan Seminar on Continuum-Mechanical and Statistical Approaches in the Mechanics of Granular Materials*, Tokyo, pp. 208–217.
- Ottino, J.M., Khakhar, D.V., 2000. Mixing and segregation of granular materials. *Annu. Rev. Fluid Mech.* 32, 55–91.
- Savage, S.B., Dai, R., 1993. Studies of granular shear flows: Wall slip velocities, 'layering' and self-diffusion. *Mech. Mater.* 16, 225–238.
- Savage, S.B., Jeffrey, D.J., 1981. The stress tensor in a granular flow at high shear rates. *J. Fluid Mech.* 110, 255–272.
- Savage, S.B., Mckeown, S., 1983. Shear stress developed during rapid shear of dense concentrations of large spherical particles between concentric cylinders. *J. Fluid Mech.* 127, 453–472.
- Savage, S.B., Sayed, M., 1984. Stresses developed by dry cohesionless granular materials sheared in an annular shear cell. *J. Fluid Mech.* 142, 391–430.
- Scott, A.M., Bridgewater, J., 1976. Self-diffusion of spherical particles in a simple shear apparatus. *Powder Technol.* 14, 177–183.
- Sudah, O.S., Coffin-Beach, D., Muzzio, F.J., 2002. Quantitative characterization of mixing of free-flowing granular material in tote (bin)-blenders. *Powder Technol.* 126, 191–200.
- Walton, O.R., Braun, R.L., 1986. Stress calculations for assemblies of inelastic spheres in uniform shear. *Acta Mech.* 63, 73–86.
- Wang, D.G., Campbell, C.S., 1992. Reynolds analogy for a shearing granular materials. *J. Fluid Mech.* 244, 527–546.
- Zhang, Y., Campbell, C.S., 1992. The interface between fluid-like and solid-like behaviour in two-dimensional granular flows. *J. Fluid Mech.* 237, 541–568.
- Zhou, Y.C., Yu, A.B., Bridgewater, J., 2003. Segregation of binary mixture of particles in a bladed mixer. *J. Chem. Technol. Biot.* 78, 187–193.
- Zik, O., Stavans, J., 1991. Self-diffusion in granular flows. *Europhys. Lett.* 16, 255–258.